Chemical Engineering Journal 171 (2011) 1201–1208

Contents lists available at ScienceDirect

Chemical Engineering Journal

journal homepage: www.elsevier.com/locate/cej

Fast removal of ammonium ion using a hydrogel optimized with response surface methodology

Yian Zheng[a,b], Yi Liu[a,b], Aiqin Wang[a,*]

[a] Center of Eco-materials and Green Chemistry, Lanzhou Institute of Chemical Physics, Chinese Academy of Sciences, No. 18 Tianshui Middle Road, Lanzhou 730000, China
[b] Graduate University of the Chinese Academy of Sciences, Beijing 100049, China

ARTICLE INFO

Article history:
Received 7 March 2011
Received in revised form 7 May 2011
Accepted 9 May 2011

Keywords:
Adsorption
Ammonium ion
Box–Behnken design
Hydrogel
Response surface methodology

ABSTRACT

Response surface methodology (RSM) based on a three-level, three-variable, Box–Behnken design (BBD) was used to optimize the preparation parameters of a hydrogel consisted of polyvinyl alcohol (PVA), acrylic acid (AA) and tourmaline (Tm). With the adsorption capacity for ammonium ion (NH_4^+) as the response, the effects of three variables, i.e. neutralization degree (ND) of AA, ratio of PVA to AA, and ratio of Tm to AA, were investigated. The predicted appropriate preparation conditions for the hydrogel were ND of AA of 70%, PVA:AA of 0.0833 and Tm:AA of 0.5, under which a hydrogel was prepared and used as the adsorbent to remove NH_4^+. The effects of contact time, ion strength, NH_4^+ concentration, temperature, and pH value on the adsorption capacity were investigated using a batch experiment. The results indicated that the as-prepared hydrogel showed entangled three-dimensional network and had the advantages of fast adsorption rate and high adsorption capacity for NH_4^+ in a pH range from 3.0 to 8.0. The regeneration and reusable experiments were also performed, and it was observed that the as-prepared hydrogel was stable and regenerable using strong acid (HCl) or base (NaOH) as the desorbing agents.

1. Introduction

Hydrogels are three-dimensional crosslinked polymeric networks and receiving great interest due to their promising applications such as sensors, separation membranes, adsorbents, and materials in medicine and pharmacy as drug delivery systems, in solving some ecological and biological problems as well as in modern technologies [1]. Hydrogels possess functional groups that can be easily ionized and hence repulse each other, by which more water molecules are captured. The higher water content and porous three-dimensional structured network can diminish the mass transfer resistance, allowing thus the solute to diffuse easily through the hydrogel structure [2]. Moreover, the presence of ionized functional groups affords the hydrogels to absorb and trap many kinds of pollutants with the opposite ionic charges. Therefore, hydrogels as the potential adsorbents have attracted much attention in recent years for the removal of cationic pollutants, such as heavy metals [3,4], dyes [5,6] and ammonium ion (NH_4^+) [2,7].

Anionic hydrogels such as polyacrylate are the most widely used adsorbents for removing toxic pollutants or recovering precious metal ions from an aqueous solution. Xie et al. studied the adsorption behaviors of a hydrogel made from acrylic acid and acrylamide and found that the maximum adsorption capacities for Cu^{2+} and Fe^{3+} were 247 and 173 mg/g [8]. Li et al. obtained a macroporous, hydrophobically modified poly(acrylic acid-acrylamide) hydrogel using poly(ethylene glycol) as the pore-forming agent, and found that this hydrogel can be used as an effective adsorbent for the removal of cationic dyes, crystal violet and basic magenta [9]. By consideration of the limitations of pure polymeric hydrogels, such as poor gel strength and stability, some studies have focused on clay incorporation into the hydrogel network to prepare organic-inorganic hydrogel. Kaşgöz et al. obtained a hydrogel–clay nanocomposite using acrylamide and 2-acrylamido-2-methylpropane sulfonic acid sodium salt as the organic monomers and montmorillonite as the inorganic component, and found that the incorporation of a low amount of clay (10 wt%) into the polymeric network increased the adsorption rate and capacity for heavy metals [3]. Our previous studies revealed that owing to the unique reducing ability of biotite, a poly(acrylic acid)/biotite hydrogel could be prepared at room temperature via a self-induced redox reaction, and the resulting hydrogel showed higher adsorption capacity for NH_4^+ [10]. Considering the biodegradability of traditional hydrogel, it was promising to prepare hydrogels that gave the required performance profile combined with environmental friendliness. Starch, chitosan, cellulose and humic acid had been used as the backbones to graft

* Corresponding author. Tel.: +86 931 4968118; fax: +86 931 8277088.
E-mail addresses: aqwang@lzb.ac.cn, aqwang@licp.cas.cn (A. Wang).

1385-8947/$ – see front matter © 2011 Elsevier B.V. All rights reserved.
doi:10.1016/j.cej.2011.05.026

acrylic acid, obtaining a series of biocompatible and biodegradable hydrogels, which showed high affinity to many kinds of cationic pollutants [11–14].

Hydrogel can be prepared by simultaneous copolymerization and crosslinking of one or more functional monomers. Most optimization studies during the development of a novel hydrogel involve variation of one factor at a time, keeping all other factors constant [15–17]. This traditional optimization method is time-consuming and expensive. Today, a statistical-based technique of response surface methodology (RSM) is used extensively to elucidate the interaction between reaction parameters for optimization. RSM is a technique whereby reaction parameters are varied simultaneously in a suitable manner to generate data for development of empirical models. It is a faster and more economical analytical approach than the traditional one, and has been applied successfully for the optimization of medium components in submerged culture of *Aspergillus flavus* for enhanced heparinase production [18], Orange II photocatalytic degradation [19], lipase-catalyzed synthesis of betulinic acid ester [20], determination of enzyme kinetic constants [21], coagulation–flocculation process for palm oil mill effluent [22], preparation of uniform silicon dioxide nanoparticles [23] and, some adsorption parameters for removing heavy metals, such as Cu^{2+}, Pb^{2+} and Cd^{2+} [24–26]. However, to the best of our knowledge, little information was reported using RSM to optimize the process parameters for obtaining hydrogels with desired properties specific to a particular application.

Acrylic acid (AA) is the mostly used functional monomer to prepare the hydrogels [15–17]. Polyvinyl alcohol (PVA) has been widely explored as water-soluble polymers for numerous biomedical and pharmaceutical applications due to its advantages of non-toxic, non-carcinogenic and bioadhesive properties [27,28]. Tourmaline (Tm) belongs to the group of silicate minerals called cyclosilicates. The general chemical formula of the tourmaline group, as a whole, can be expressed as XY_3Z_6–$(T_6O_{18})(BO_3)_3V_3W$, where X = Na^+, Ca^{2+}, K^+, or vacancy, Y = Li^+, Fe^{2+}, Mg^{2+}, Fe^{3+}, Al^{3+}, Cr^{3+}, V^{3+}, (Ti^{4+}), Z = Al^{3+}, Fe^{3+}, Mg^{2+}, Cr^{3+}, V^{3+}, (Fe^{2+}), T = Si^{4+}, Al^{3+}, (B^{3+}), B = B^{3+} or vacancy, V = [O(3)] = OH^-, O^{2-}, W = [O(1)] = OH^-, O^{2-}, F^- and metal ions in () indicate minor or possible substitution [29]. Based on these information, we prepared a series of hydrogels based on AA, PVA and Tm. The present study is an attempt to optimize the preparation process of PVA/PAA/Tm hydrogel using RSM, with the adsorption capacity of resulting hydrogel for NH_4^+ (an important pollutant promoting eutrophication) as the reference. The parameters that need to be optimized are neutralization degree (ND) of AA, ratio of PVA:AA, and ratio of Tm:AA. When the preparation parameters were chosen, a hydrogel with desired properties was obtained and used as the adsorbent to remove NH_4^+ using batch adsorption experiments. The adsorption kinetics, adsorption isotherms, pH effect, desorption and reusability were investigated and evaluated.

2. Materials and methods

2.1. Materials

Acrylic acid (AA, chemically pure, Sinopharm Chemical Reagent Co., Ltd., Shanghai, China) was distilled under reduced pressure before use. Ammonium persulfate (APS, analytical grade, Sinopharm Chemical Reagent Co., Ltd., Shanghai, China), *N*,*N*′-methylene-bisacrylamide (MBA, chemically pure, Shanghai Yuanfan Additives Plant, Shanghai, China), polyvinyl alcohol (PVA with the average polymerization degree of 1700 and alcoholysis degree of 99%, Lanzhou Vinylon Factory, Lanzhou, China) were used as received. Tourmaline (Tm, Jinjianshi Nano Technology Co., Ltd., Hebei, China) was milled through a 200-mesh screen prior to use.

Table 1
Experimental ranges and levels of the independent variables.

Variables	Ranges and levels		
	−1	0	+1
X_1, ND of AA (%)	20	50	80
X_2, PVA:AA	0.0833	0.104	0.125
X_3, Tm:AA	0	0.25	0.50

All other agents used were of analytical grade and all solutions were prepared with distilled water.

2.2. Preparation of PVA/PAA/Tm hydrogel

In a four-neck flask equipped with a stirrer, a condenser, a thermometer and a nitrogen line, an appropriate amount of PVA was dispersed in 60 mL distilled water and heated to 80 °C under stirring until PVA was dissolved completely. Then the temperature was lowered to 70 °C while 4 mL solution containing 0.2 g APS was added dropwise for 10 min. After that, a premixed solution containing 20 mL distilled water, 0.3 g MBA, 7.2 g AA with different ND and an appropriate amount of Tm was added dropwise into the flask from a constant pressure funnel. Nitrogen atmosphere was kept throughout the experiments. The solution was stirred at 70 °C for 3 h to complete the polymerization reaction, and the resulting hydrogel was immersed in distilled water to remove any impurities present and then dehydrated with ethanol. Finally, the product was dried at 70 °C and the hydrogel adsorbent used during the adsorption process was milled through a 40–80 mesh screen.

2.3. Experimental design

The Box–Behnken factorial design was used to optimize the preparation parameters with adsorption capacity of resulting hydrogel for NH_4^+ as the response. Since different variables are usually expressed in different units and/or have different limits of variation, the significance of their effects on response can only be compared after they are coded. For statistical calculations, the variable X_i was coded as x_i according to the following equation:

$$x_i = \frac{X_i - X_0}{\Delta X_i} \quad (1)$$

where X_i is the real value of the ith independent variable, X_0 is the real value of an independent variable at the centre point and ΔX_i is the step change. ND of AA (X_1), PVA:AA ratio (X_2) and Tm:AA ratio (X_3) were chosen as three independent variables during the preparation process. Their range and levels were listed in Table 1. The adsorption capacity for NH_4^+ was selected as the dependent variable. The response variable was fitted by a second-order model in the form of quadratic polynomial equation:

$$Y = \beta_0 + \sum \beta_i x_i + \Sigma \beta_{ii} x_i^2 + \sum \beta_{ij} x_i x_j \quad (2)$$

where Y is the response variable to be modeled; β_0, β_i, β_{ii} and β_{ij} are constant regression coefficient of the model; x_i and x_j ($i = 1 \rightarrow 3$; $j = 1 \rightarrow 3$; $i \neq j$) represent the independent variables in the form of coded values. The actual design of this work was presented in Table 2. Based on this table, the experiments were conducted for obtaining the response, i.e. adsorption capacity for NH_4^+, at the corresponding independent variables addressed in the experimental design matrix by applying quadratic model. The parameters of the response equations and corresponding analysis on variables were evaluated using Design Expert Software Version 7.1.3 (STAT-EASE Inc., Minneapolis, USA).

Table 2
BBD and results for the study of three experimental variables in coded units.

Run	Variables (coded)			NH_4^+ adsorbed (mg N/g)	
	x_1	x_2	x_3	Experimental	Predicted
1	0	1	−1	30.81	32.49
2	1	0	1	27.99	26.64
3	1	1	0	27.91	27.37
4	0	0	0	30.02	30.02
5	−1	1	0	28.10	25.07
6	0	0	0	30.02	30.02
7	0	−1	1	31.71	30.03
8	0	0	0	30.02	30.02
9	0	1	1	24.76	26.65
10	0	−1	−1	33.81	31.92
11	−1	−1	0	18.99	19.52
12	−1	0	1	17.39	18.54
13	1	−1	0	32.69	35.73
14	0	0	0	30.02	30.02
15	−1	0	−1	19.89	21.25
16	0	0	0	30.02	30.02
17	1	0	−1	32.81	31.66

2.4. Adsorption experiment

NH_4^+ adsorption experiments were performed under 120 rpm with an orbital shaker THZ-98A. The experiments were carried out in a series of 50 mL conical flasks containing 0.05 g hydrogel adsorbent and 25 mL NH_4^+ solutions. On reaching equilibrium the adsorbent was separated and the NH_4^+ concentration in the solution was measured according to Nessler's reagent colorimetric method. The adsorption capacity of the as-prepared hydrogel for NH_4^+ was calculated from the following equation:

$$q_e = \frac{(C_0V_1 - C_eV_2)}{m} \quad (3)$$

where q_e is the adsorption capacity of NH_4^+ onto adsorbent (mg N/g), C_0 is the initial NH_4^+ concentration (mg N/L), C_e is the equilibrium NH_4^+ concentration (mg N/L), m is the mass of adsorbent used (mg), and V_1 and V_2 are the volumes of NH_4^+ solution before and after the adsorption (mL). All assays were carried out in triplicate. The limit of adsorption experimental error was ±5%.

For the adsorption kinetic studies, a series of solutions containing 100 mg N/L NH_4^+ were allowed to contact with 0.05 g hydrogel. At different intervals (1, 2, 5, 10, 30, and 60 min), 1 mL aliquot was sampled and analyzed for residual NH_4^+ concentration. During this process, the influences of ion strength on the adsorption capacity were also investigated in the solution containing 100 mg N/L NH_4^+ and different NaCl concentrations (0, 1, and 5 mmol/L). To investigate the adsorption isotherms at different temperature (30 °C, 40 °C, and 50 °C), a series of NH_4^+ solutions with different concentration (13–130 mg N/L) were kept in contact with 0.05 g hydrogels for 30 min at natural pH (6.0–7.0). The effects of pH on NH_4^+ adsorption were studied at 100 mg N/L NH_4^+ with different pH values (2.0–10.0) and contact time of 30 min. When the adsorption process was complete, the pH values after the adsorption were also recorded.

2.5. Desorption and reusability

A fixed amount (0.05 g of dried weight) of NH_4^+-loaded hydrogel was contacted, respectively, with 25 mL solution with different pH values and agitated for 30 min at 30 °C/120 rpm. The desorbed amount of NH_4^+ was then obtained, and accordingly, an appropriate eluent was selected. Once an eluent was chosen, it is important to evaluate the reusability of an adsorbent from the viewpoint of practical application. Typically, the recovered hydrogel was washed with distilled water for several times for another adsorption. A similar procedure was repeated and the adsorption capacity after several times was then achieved.

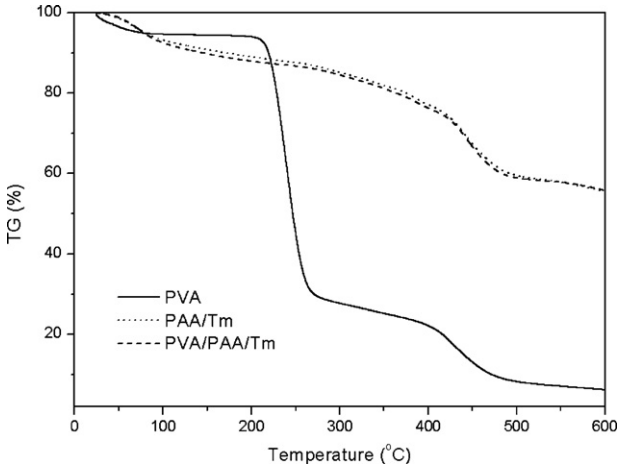

Fig. 1. TG curves of PVA, PAA/Tm and PVA/PAA/Tm.

2.6. Characterization

FTIR was conducted on the Thermo Nicolet NEXUS TM spectrophotometer using KBr pellets. The thermal behaviors of PVA, PAA/Tm and PVA/PAA/Tm were evaluated on a Perkin Elmer instrument at a heating rate of 10 °C/min using dry nitrogen purge at a flow rate of 200 mL/min. The surface morphologies of the samples were examined using a JSM-5600 scanning electron microscope (SEM) with gold film.

3. Results and discussion

3.1. Characterization of PVA/PAA/Tm

FTIR analysis (data not shown) indicates that after the reaction, some characteristic absorption bands of PVA, Tm and PAA can be reflected in the spectrum of PVA/PAA/Tm with no new absorption bands appearing, an implication of the formation of PVA/PAA/Tm hydrogel. It is observed from Fig. 1 that the major weight loss of PVA is located at 241 °C. However, TG curves of PAA/Tm and PVA/PAA/Tm show a similar lower weight loss over the temperature studied. Then, we can conclude that the thermal stability of PVA/PAA/Tm is not decreased by the introduction of PVA into the hydrogel. The surface morphologies of PVA/PAA/Tm hydrogel are shown in Fig. 2. It is clearly observed that PVA/PAA/Tm shows an entangled three-dimensional structured network with many interconnected pores. Inside these pores, some lines as the stripes on a leaf are visible. One can anticipate that this coarse, porous surface is beneficial for an adsorption process.

3.2. Optimization of preparation parameters

The adsorption capacities of PVA/PAA/Tm for NH_4^+ are summarized in Table 2. The following equation is a regression model with the experimental results:

$$Y = 30.02 + 4.63x_1 - 0.70x_2 - 1.93x_3 - 3.47x_1x_2 - 0.58x_1x_3 - 0.99x_2x_3 - 4.43x_1^2 + 1.33x_2^2 - 1.07x_3^2 \quad (4)$$

Statistical testing of the model was preformed with the Fisher's statistical test for analysis of variance (ANOVA), as shown in Table 3. The significance of each model is assessed from the coefficient (R^2)

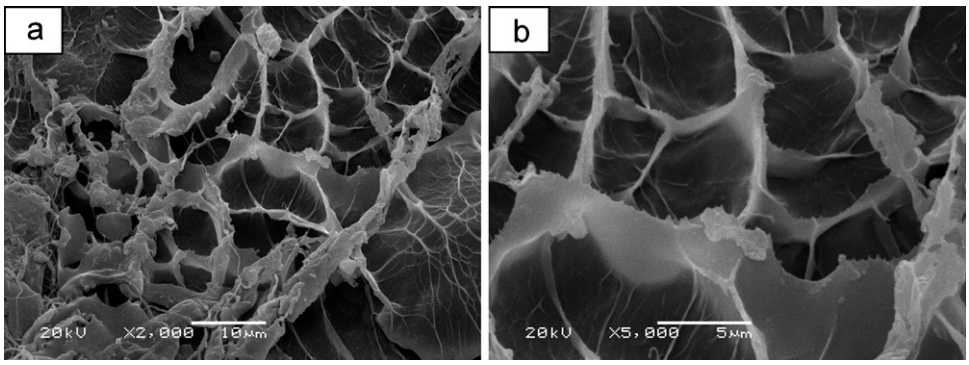

Fig. 2. SEM micrographs of PVA/PAA/Tm with different magnification of (a) 2000× and (b) 5000×.

which is found to be 0.9025, implying that only 9.75% of the variation in Y response cannot be explained by this model. The model F value of 7.20 implies that the model is significant. The significance of each term in this model is also evaluated by P value (Prob > F). If a P value is lower than 0.05, it means that the term is significant at 95% confidence level. According to the ANOVA analysis, it is observed that x_1, x_1x_2 and x_1^2 are significant model terms. In usual cases, the term with $P > 0.05$ can be omitted from the model. However, in this study, the insignificant terms are still maintained to support the hierarchical nature of this model [30]. Obviously, ND of AA plays an important role in controlling the final adsorption capacity for NH_4^+ during the preparation process, suggesting that the electrostatic attraction between negatively charged $-COO^-$ groups and positively charged NH_4^+ may dominate the entire adsorption process. The changes in ND of AA can alter the number of carboxylate groups ($-COO^-$), and thus would produce some impressive effects on the adsorption capacity. Then, RSM can, in some extent, reveal the possible mechanism for the adsorption of NH_4^+ onto the as-prepared hydrogel.

From the regression Eq. (4), the optimal preparation conditions for PVA/PAA/Tm were obtained as follows: ND of AA of 80%, PVA:AA of 0.09 and Tm:AA of 0, under which the as-prepared hydrogel is expected to have maximum adsorption capacity for NH_4^+ (34.73 mg N/g). Though the "best" response is found, the resulting adsorbent material is very soft and easily deformable upon contact, which makes it unsuitable for practice. In order to obtain a hydrogel with higher adsorption capacity and hydrogel strength, a compromise is applied using the "point prediction" function of the BBD, that is, we find factor settings that can satisfy the practical demands, as follows: ND of AA of 70%, PVA:AA of 0.0833 and Tm:AA of 0.5. In the current study, the addition of Tm into the hydrogel can (i) reduce the production cost as Tm is abundant and inexpensive, (ii) enhance the hydrogel strength as more Tm particles will act as physical fillers in the hydrogel, and (iii) reduce the swelling degree.

Table 3
Analysis of variance for the response of the adsorption capacity for NH_4^+.

Source	Sum of squares	Degrees of freedom	Mean squares	F value	P value Prob > F
Model	352.90	9	39.21	7.20	0.0082
x_1	171.43	1	171.43	31.49	0.0008
x_2	3.95	1	3.95	0.73	0.4226
x_3	29.87	1	29.87	5.49	0.0516
x_1x_2	48.30	1	48.30	8.87	0.0206
x_1x_3	1.35	1	1.35	0.25	0.6343
x_2x_3	3.91	1	3.91	0.72	0.4248
x_1^2	82.48	1	82.48	15.15	0.0060
x_2^2	7.40	1	7.40	1.36	0.2818
x_3^2	4.85	1	4.85	0.89	0.3764
Residual	38.11	7	5.44		
Corrected total	391.01	16			

R^2, 0.9025; CV, 8.32.

For an adsorption process, lower swelling degree is more beneficial. By a comprehensive consideration of alternative experimental criteria, we select the experimental conditions as above. Under the chosen conditions, the adsorption capacity of hydrogel for NH_4^+ is predicted to be 33.08 mg N/g using RSM. To verify the theoretical value, a hydrogel was prepared under these chosen conditions and its adsorption capacity was determined to be 32.06 mg N/g for NH_4^+, closer to the predicted value.

With adsorption capacity for NH_4^+ as the response, the three-dimensional response surfaces are shown in Fig. 3. It is clear that the adsorption capacity for NH_4^+ is sensitive to the changes in ND of AA, while PVA:AA and Tm:AA have insignificant effects. This can be attributed to that increase in ND of AA can give a large amount of negatively charged carboxylate groups, i.e. $-COO^-$, which can increase the number of available adsorption sites for NH_4^+, and thus improve the adsorption capacity.

3.3. Adsorption kinetics

Adsorption kinetics, indicating the adsorption rate, is an important characteristic of an adsorbent. The adsorption process at different ion strength is rapid in the initial 10 min at that time it reaches equilibrium (Fig. 4), which means a quite fast adsorption process. This is because that the as-prepared adsorbent is consisted of flexible polymeric chains with super-hydrophilic characteristics. When it is immersed in an aqueous solution, water molecules penetrate quickly into the hydrogel, resulting in a dimensional increase of polymeric networks. Then, the concentration gradient of NH_4^+ is formed at gel–water interface, and the diffusion of NH_4^+ into the gel is started. Due to the presence of a large amount of negatively charged $-COO^-$ groups, NH_4^+ moved from the external solution into the hydrogel can be adsorbed and trapped within the polymeric network, leading the adsorption system to reach equilibrium within a few minutes.

The effects of ion strength on the adsorption capacity of NH_4^+ onto the hydrogel were also studied as a function of contact time. Background electrolytes used in this study were 1 and 5 mmol/L NaCl, as shown in Fig. 4. Obviously, the addition of NaCl in the adsorption system has some effects on the adsorption capacity for NH_4^+, especially at the initial adsorption stage. This is derived from a screening effect of the surface charge produced by the salt addition [31]. Generally, when the electrostatic interaction between the surface and the adsorptive ion is repulsive, an increase in the ion strength will increase the adsorption capacity. Conversely, when the electrostatic interaction is attractive, an increase of the ion strength will diminish the adsorption capacity. In this study, the governed adsorption mechanism between the adsorbent and adsorbate is ascribed to the negatively charged $-COO^-$ groups and positively charged NH_4^+, and thus the screening effect of the surface charge would result in a decrease in the adsorption capacity.

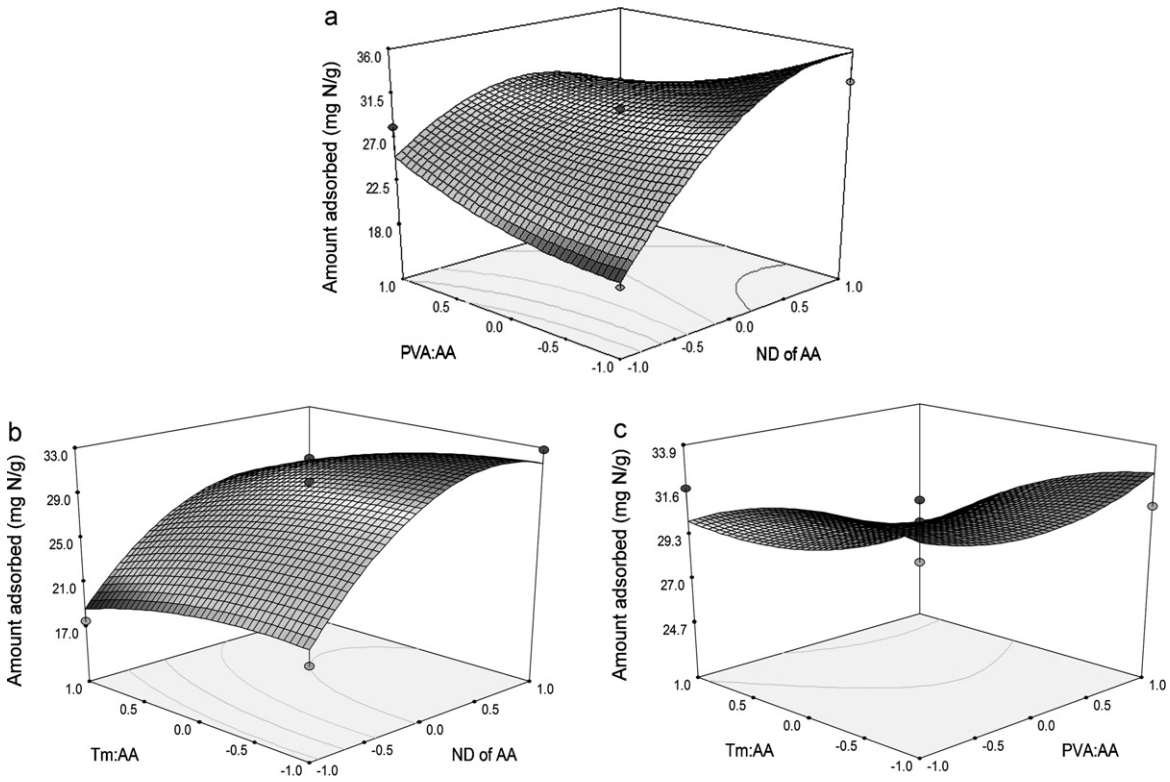

Fig. 3. Response surface graphs of adsorption capacity showing the effect of variables of (a) x_1–x_2, (b) x_1–x_3, and (c) x_2–x_3.

In order to make a comparison, in this study, we used the pseudo-second-order kinetic model to obtain the initial adsorption rate for NH_4^+:

$$\frac{t}{q} = \frac{1}{k_2 q_e^2} + \frac{t}{q_e} \quad (5)$$

where q_e and q are the adsorption capacity (mg N/g) at equilibrium and at time t (min), respectively; k_2 (g/(mg min)) denotes the rate constant of the pseudo-second-order model for adsorption. The slope and intercept of the linear plot of t/q against t yield the values of q_e and k_2. The initial adsorption rate h (mg/(g min)) can be determined using the equation of $h = k^2 q_e^2$. These parameters were summarized in Table 4. The calculated q_e values agree well with the experimental q_e values, and also, the correlation coefficients R^2 for the second-order kinetic plots at different ion strength are above 0.99, indicating that the second-order kinetic model can describe the experimental data. That is, the adsorption capacity of this hydrogel for NH_4^+ is related to the availability of its adsorption sites on the surface. In addition, it is observed from Table 4 that the presence of NaCl in the adsorption system would produce negative effects on the initial adsorption rate.

3.4. Adsorption isotherms

Fig. 5 shows the results of NH_4^+ adsorption isotherm, the relationship between the amount of NH_4^+ adsorbed per unit mass of the hydrogel (q_e, mg N/g) and its final concentration in the solution (C_e). The plot of NH_4^+ adsorption against equilibrium concentra-

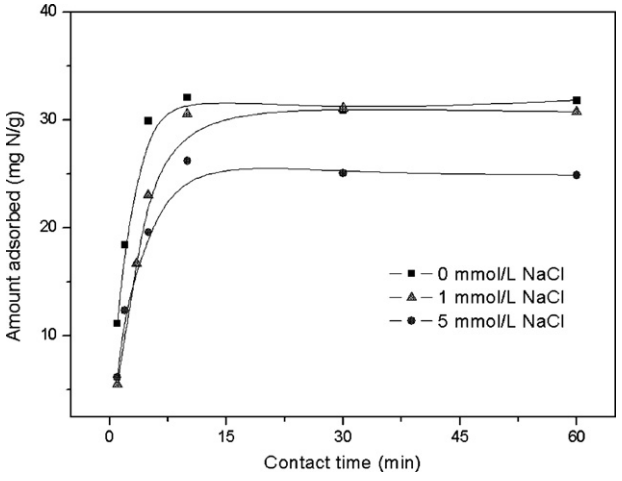

Fig. 4. Variation in the adsorption capacity of NH_4^+ onto the hydrogel as a function of contact time and ion strength: C_0 = 100 mg N/L, m/V = 2 g/L, and T = 30 °C.

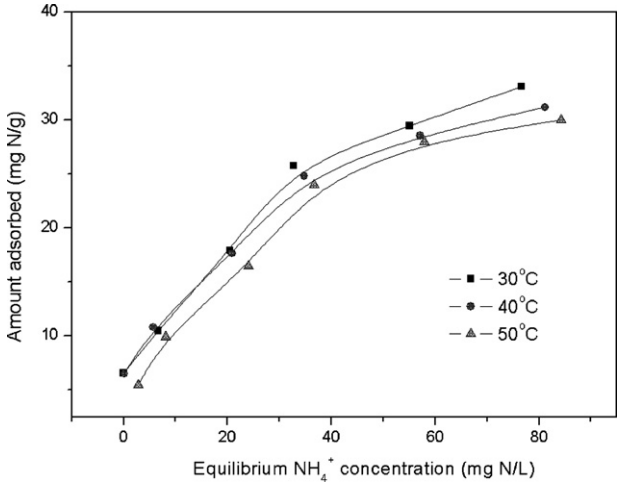

Fig. 5. Adsorption isotherms of NH_4^+ onto the hydrogel: t = 30 min, m/V = 2 g/L, and T = 30 °C.

Table 4
Kinetic parameters for NH_4^+ adsorption by PVA/PAA/Tm hydrogel.

Pseudo-second-order model	q_e, exp (mg N/g)	q_e, cal (mg N/g)	k_2 (g/mg/min)	h	R^2
0 mmol/L NaCl	32.06	32.36	2.87×10^{-2}	30.10	0.9996
1 mmol/L NaCl	30.79	32.57	1.15×10^{-2}	12.23	0.9977
5 mmol/L NaCl	25.38	25.84	2.30×10^{-2}	15.38	0.9987

Table 5
Langmuir and Freundlich constants and correlation coefficients for the adsorption of NH_4^+ onto the as-prepared hydrogel.

Temperature	Langmuir			Freundlich		
	q_m (mg N/g)	b (L/mg)	R^2	K (L/g)	n	R^2
30 °C	42.74	0.04268	0.9874	4.323	2.081	0.9823
40 °C	33.78	0.09730	0.9617	4.095	9.556	0.9169
50 °C	37.74	0.04498	0.9768	1.921	3.278	0.9887

tion indicates that the adsorption capacity considerably increases with increasing the NH_4^+ concentration if $C_e < 40$ mg N/L, beyond that the increase of the adsorption capacity is less significant.

Fitting of adsorption isotherm equations to experimental data is often an important aspect of data analysis. In this study, typical isotherms, i.e. Langmuir and Freundlich models [32,33], were used for fitting the adsorption experimental data:

$$\text{Langmuir equation}: \frac{C_e}{q_e} = \frac{1}{q_m b} + \frac{C_e}{q_m} \quad (6)$$

$$\text{Freundlich equation}: \log(q_e) = \frac{1}{n}\log(C_e) + \log K \quad (7)$$

where q_e is the equilibrium adsorption capacity of NH_4^+ onto adsorbent (mg N/g), C_e is the equilibrium NH_4^+ concentration (mg N/L), q_m is the monolayer adsorption capacity (mg N/g), b is the Langmuir adsorption constant (L/mg) and, K (L/g) and n (dimensionless) are Freundlich isotherm constants. These parameters can be determined by linear regression of the experimental data. The estimated model parameters with correlation coefficient (R^2) are summarized in Table 5. It is evident that compared with Freundlich model, Langmuir model can well describe the experimental data, and the calculated monolayer adsorption capacity q_m for NH_4^+ is found to be 42.74, 33.78 and 37.74 mg N/g at 30 °C, 40 °C and 50 °C, respectively. Lower temperature seems to be beneficial for the NH_4^+ adsorption onto the hydrogel.

3.5. pH-dependence

Generally, pH value is one of the most important parameters affecting the adsorption process. In order to determine the effects of pH values on NH_4^+ adsorption, experiments were carried out using various pH levels in the range of 2.0–10.0, as shown in Fig. 6. It appears that the adsorption capacity shows a remarkable increase with increasing pH from 2.0 to 3.0, and then the adsorption capacity remains almost a constant within the pH range of 3.0–8.0. Further increase in pH values would decrease the adsorption capacity for NH_4^+, especially at higher pH, such as pH 10.0. In this study, the presence of $-COO^-$ groups on the adsorbent has a vital role in controlling the adsorption capacity for NH_4^+. pK_a of PAA is about 4.7 [34], then the carboxylic acid groups can be easily ionized above pH 4.7. Due to the rapid adsorption of NH_4^+ onto the as-prepared hydrogel, the equilibrium pH value is considered to be the governed factor influencing the ionization degree of –COOH groups, and accordingly, the final adsorption capacity for NH_4^+ is affected. As shown in Fig. 6, after the adsorption, the equilibrium pH values keep almost a constant within pH range of 3.0–8.0. This behavior is ascribed to the buffer action of –COOH and $-COO^-$ groups, a typical characteristic of a hydrogel consisting mainly of PAA [35,36]. However, in the stronger acidic region, some $-COO^-$ groups are transformed to –COOH groups, leading the electrostatic attraction between adsorbent and adsorbate to diminish, and accordingly, the adsorption capacity decreases. At higher pH values, NH_4^+ is neutralized by hydroxyl ion rendering it uncharged [37], together with increased ion strength, resulting in a decreasing adsorption capacity for NH_4^+. Nevertheless, the as-prepared hydrogel can still be considered as an excellent candidate for removing NH_4^+ due to its wide pH application range.

Fig. 7 shows the FTIR spectra before and after the adsorption for NH_4^+ at different pH values. It can be observed that after adsorption at pH 2.0, there appears some characteristic stretching bands of –COOH and $-COO^-$ groups lying, respectively, at 1717, 1542 and 1403 cm^{-1}. With increasing pH value from 2.0 to 3.0, the stretching vibration of –COOH groups gets weakened and the intensities of asymmetric/symmetric vibration absorption bands of $-COO^-$ groups show a gradual increase. Afterwards, it appears that the latter absorption bands remain unchangeable until pH 8.0. A further increase of pH value leads to disappearing stretching vibration of –COOH groups. That is to say, at this point, all of –COOH groups have transformed to $-COO^-$ groups. FTIR analysis results are consistent with that obtained from pH effects, confirming that the electrostatic attraction between $-COO^-$ groups and NH_4^+ can describe the main adsorption process. Also, this would explain the observed maximum, constant adsorption capacity for NH_4^+ within pH range of 3.0–8.0.

3.6. Desorption and reusability

Desorption studies can help elucidating the mechanism of an adsorption process. If the NH_4^+ adsorbed onto the adsorbent can

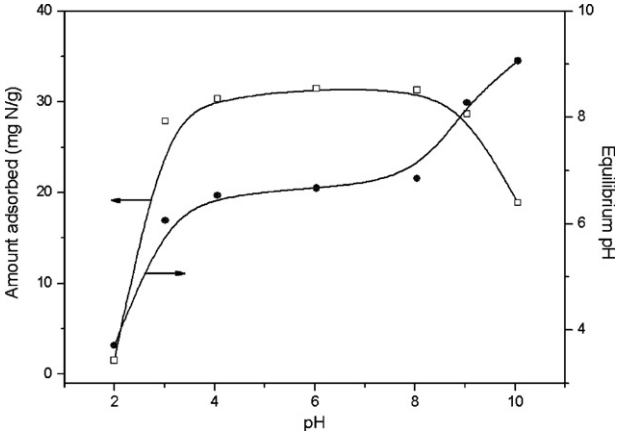

Fig. 6. Effect of solution pH on NH_4^+ adsorption: $C_0 = 100$ mg N/L, $t = 30$ min, $m/V = 2$ g/L, and $T = 30$ °C.

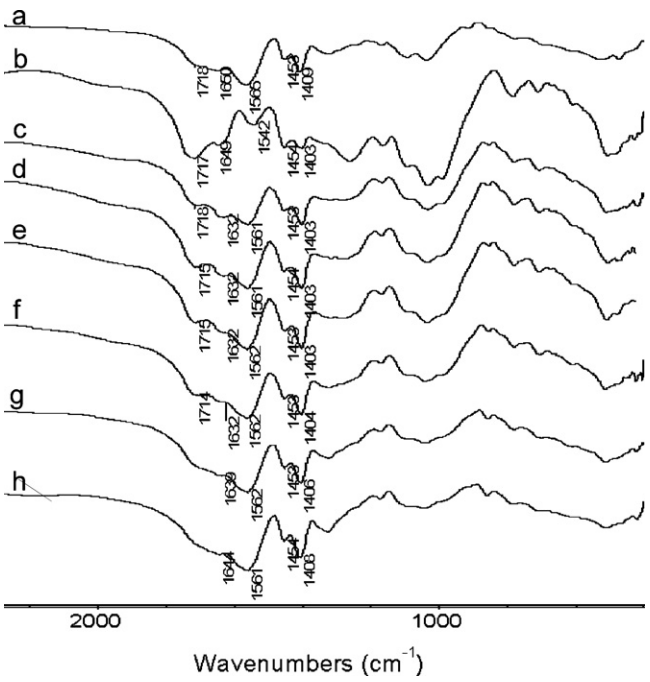

Fig. 7. FTIR of the hydrogel before (a) and after the adsorption (b–h): (b) pH 2.0, (c) pH 3.0, (d) pH 4.0, (e) pH 6.0, (f) pH 8.0, (g) pH 9.0, and (h) pH 10.0.

be desorbed by water, it can be said that the attachment of NH_4^+ onto the adsorbent is by weak bonds. If the strong acid or base, such as HCl or NaOH can desorb the NH_4^+, it can be said that the attachment of NH_4^+ onto the adsorbent is by ion exchange or electrostatic attraction [38]. In this study, the desorption of adsorbed NH_4^+ onto the as-prepared hydrogel was studied using a series of solutions with different pH values, as shown in Fig. 8. It is clear that the strong acid ($pH \leq 2$) or strong base ($pH \geq 12$) can give the higher recovery of NH_4^+, suggesting that the adsorption of NH_4^+ onto this hydrogel is mainly controlled by electrostatic attraction, consistent with the conclusions obtained above.

An adsorbent, in addition to its good adsorption and desorption characteristics, must also exhibit a good regeneration ability for multiple uses. Here, we used 0.1 mol/L NaOH as the desorbing agent to study the reusability of the as-prepared hydrogel for NH_4^+ adsorption. After five adsorption–desorption cycles, no obvious loss in the adsorption capacity is observed, suggesting that the recovered hydrogel shows an excellent reusability for NH_4^+ adsorption. Though 0.1 mol/L NaOH is chosen as the desorbing agent, there is no any degradation for hydrogel after reusing. This is ascribed to that the adsorbent has a completely crosslinked three-dimensional structure and its preparation process involves the breakage and formation of chemical bonds. Thus, the resulting hydrogel is resistant to NaOH as the desorbing agent and stable after the reusing.

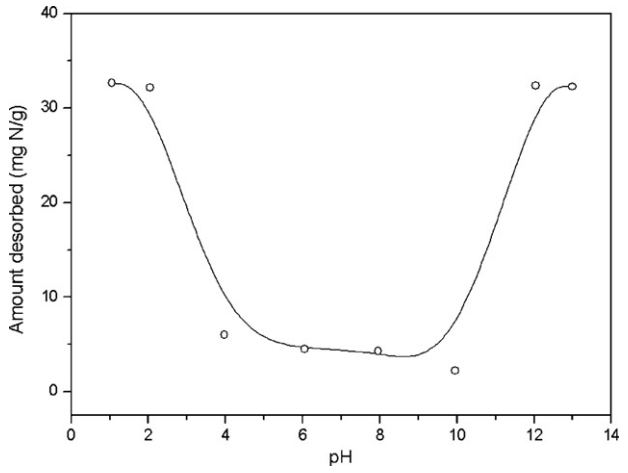

Fig. 8. Effect of pH on the desorption of NH_4^+ from hydrogel. Adsorption conditions: $C_0 = 100$ mg N/L, $t = 30$ min, $m/V = 2$ g/L, and $T = 30\,^\circ$C; desorption conditions: $t = 30$ min, $m/V = 2$ g/L, and $T = 30\,^\circ$C.

4. Conclusions

Response surface methodology was applied for optimizing the preparation parameters to obtain a hydrogel with excellent adsorption properties for NH_4^+. The statistical analysis results show that the appropriate preparation conditions are as follows: ND of AA of 70%, PVA:AA of 0.0833 and Tm:AA of 0.50. Among three parameters, ND of AA is the most important one in controlling the final adsorption capacity. Batch adsorption experiments indicate that the adsorption equilibrium can be achieved within 10 min and the monolayer adsorption capacity is 42.74, 33.78 and 37.74 mg N/g at 30 °C, 40 °C and 50 °C, respectively, meaning fast adsorption rate and high adsorption capacity of the as-prepared hydrogel for NH_4^+. In a pH range of 3.0–8.0, the as-prepared hydrogel shows appreciable constant adsorption capacity for NH_4^+. The NH_4^+ adsorbed can be easily desorbed by strong acid or strong base and the recovered hydrogel shows excellent reusability.

Acknowledgement

This work is supported by the National Natural Science Foundation of China (No. 20877077).

References

[1] E. Karadağ, Ö.B. Üzüm, D. Saraydin, Swelling equilibria and dye adsorption studies of chemically crosslinked superabsorbent acrylamide/maleic acid hydrogels, Eur. Polym. J. 38 (2002) 2133–2141.
[2] Y. Zheng, A. Wang, Evaluation of ammonium removal using a chitosan-*g*-poly (acrylic acid)/rectorite hydrogel composite, J. Hazard. Mater. 171 (2009) 671–677.
[3] H. Kaşgöz, A. Durmuş, A. Kaşgöz, Enhanced swelling and adsorption properties of AAm-AMPSNa/clay hydrogel nanocomposites for heavy metal ion removal, Polym. Adv. Technol. 19 (2008) 213–220.
[4] X. Wang, Y. Zheng, A. Wang, Fast removal of copper ions from aqueous solution by chitosan-*g*-poly(acrylic acid)/attapulgite composites, J. Hazard. Mater. 168 (2009) 970–977.
[5] S. Ekici, Y. Işıkver, D. Saraydın, Poly(acrylamide-sepiolite) composite hydrogels: preparation, swelling and dye adsorption properties, Polym. Bull. 57 (2006) 231–241.
[6] L. Wang, J. Zhang, A. Wang, Removal of methylene blue from aqueous solution using chitosan-*g*-poly(acrylic acid)/montmorillonite superadsorbent nanocomposite, Colloids Surf. A 322 (2008) 47–53.
[7] Y. Zheng, J. Zhang, A. Wang, Fast removal of ammonium nitrogen from aqueous solution using chitosan-*g*-poly(acrylic acid)/attapulgite composite, Chem. Eng. J. 155 (2009) 215–222.
[8] J. Xie, X. Liu, J. Liang, Absorbency and adsorption of poly(acrylic acid-co-acrylamide) hydrogel, J. Appl. Polym. Sci. 106 (2007) 1606–1613.
[9] S. Li, X. Liu, T. Zou, W. Xiao, Removal of cationic dye from aqueous solution by a macroporous hydrophobically modified poly(acrylic acid-acrylamide) hydrogel with enhanced swelling and adsorption properties, Clean-Soil Air Water 38 (2010) 378–386.
[10] Y. Zheng, A. Wang, Preparation and ammonium adsorption properties of biotite-based hydrogel composites, Ind. Eng. Chem. Res. 49 (2010) 6034–6041.
[11] G. Güçlü, E. Al, S. Emik, T.B. İyim, S. Özgümüs, M. Özyürek, Removal of Cu^{2+} and Pb^{2+} ions from aqueous solutions by starch-graft-acrylic acid/montmorillonite superabsorbent nanocomposite hydrogels, Polym. Bull. 65 (2010) 333–346.
[12] Y. Zheng, D. Huang, A. Wang, Chitosan-*g*-poly(acrylic acid) hydrogel with crosslinked polymeric networks for Ni^{2+} recovery, Anal. Chim. Acta 687 (2011) 193–200.
[13] Y. Liu, W. Wang, A. Wang, Adsorption of lead ions from aqueous solution by using carboxymethyl cellulose-*g*-poly (acrylic acid)/attapulgite hydrogel composites, Desalination 259 (2010) 258–264.
[14] J.-Z. Yi, Y.-Q. Ma, L.-M. Zhang, Synthesis and decoloring properties of sodium humate/poly(N-isopropylacrylamide) hydrogels, Bioresour. Technol. 99 (2008) 5362–5367.

[15] A. Li, A. Wang, J. Chen, Studies on poly(acrylic acid)/attapulgite superabsorbent composite. I. Synthesis and characterization, J. Appl. Polym. Sci. 92 (2004) 1596–1603.
[16] Z. Chen, M. Liu, S. Ma, Synthesis and modification of salt-resistant superabsorbent polymers, React. Funct. Polym. 62 (2005) 85–92.
[17] J. Lin, J. Wu, Z. Yang, M. Pu, Synthesis and properties of poly(acrylic acid)/mica superabsorbent nanocomposite, Macromol. Rapid Commun. 22 (2001) 422–424.
[18] J. Banga, C.K.M. Tripathi, Response surface methodology for optimization of medium components in submerged culture of *Aspergillus flavus* for enhanced heparinase production, Lett. Appl. Microbiol. 49 (2009) 204–209.
[19] C. Betianu, F.A. Caliman, M. Gavrilescu, I. Cretescu, C. Cojocaru, I. Poulios, Response surface methodology applied for Orange II photocatalytic degradation in TiO_2 aqueous suspensions, J. Chem. Technol. Biotechnol. 83 (2008) 1454–1465.
[20] Y. Yasin, M. Basri, F. Ahmad, A.B. Salleh, Response surface methodology as a tool to study the lipase-catalyzed synthesis of betulinic acid ester, J. Chem. Technol. Biotechnol. 83 (2008) 694–698.
[21] İ.H. Boyacı, A new approach for determination of enzyme kinetic constants using response surface methodology, Biochem. Eng. J. 25 (2005) 55–62.
[22] A.L. Ahmad, S. Ismail, S. Bhatia, Optimization of coagulation–flocculation process for palm oil mill effluent using response surface methodology, Environ. Sci. Technol. 39 (2005) 2828–2834.
[23] H.-C. Wang, C.-Y. Wu, C.-C. Chung, M.-H. Lai, T.-W. Chung, Analysis of parameters and interaction between parameters in preparation of uniform silicon dioxide nanoparticles using response surface methodology, Ind. Eng. Chem. Res. 45 (2006) 8043–8048.
[24] K.M. Helen, R. Iyyaswami, G.P. Magesh, R.M. Lima, Modelling, analysis and optimization of adsorption parameters for H_3PO_4 activated rubber wood sawdust using response surface methodology (RSM), Colloids Surf. B 70 (2009) 35–45.
[25] M. Amini, H. Younesi, N. Bahramifar, A.A.Z. Lorestani, F. Ghorbani, A. Daneshi, M. Sharifzadeh, Application of response surface methodology for optimization of lead biosorption in an aqueous solution by *Aspergillus niger*, J. Hazard. Mater. 154 (2008) 694–702.
[26] F. Ghorbani, H. Younesi, S.M. Ghasempouri, A.A. Zinatizadeh, M. Amini, A. Daneshi, Application of response surface methodology for optimization of cadmium biosorption in an aqueous solution by *Saccharomyces cerevisiae*, Chem. Eng. J. 145 (2008) 267–275.
[27] M.J. Roberts, M.D. Bently, J.M. Harris, Chemistry for peptide and protein PEGylation, Adv. Drug Deliv. Rev. 54 (2002) 459–476.
[28] J.J. Sahlin, N.A. Peppas, Near-field FTIR imaging: a technique for enhancing spatial resolution in FTIR microscopy, J. Appl. Polym. Sci. 63 (1997) 103–110.
[29] R.R. Yeredla, H. Xu, Incorporating strong polarity minerals of tourmaline with semiconductor titania to improve the photosplitting of water, J. Phys. Chem. C 112 (2008) 532–539.
[30] I. Dahlan, K.T. Lee, A.H. Kamaruddin, A.R. Mohamed, Analysis of SO_2 sorption capacity of rice husk ash (RHA)/CaO/NaOH sorbents using response surface methodology (RSM): untreated and pretreated RHA, Environ. Sci. Technol. 42 (2008) 1499–1504.
[31] V. Lópes-Ramón, C. Moreno-Castilla, J. Rivera-Utrilla, L.R. Radovic, Ionic strength effects in aqueous phase adsorption of metal ions on activated carbons, Carbon 41 (2003) 2020–2022.
[32] A. Mittal, D. Kaur, A. Malviya, J. Mittal, V.K. Gupta, Adsorption studies on the removal of coloring agent phenol red from wastewater using waste materials as adsorbents, J. Colloid Interf. Sci. 337 (2009) 345–354.
[33] T.K. Naiya, A.K. Bhattacharya, S.K. Das, Adsorption of Cd(II) and Pb(II) from aqueous solutions on activated alumina, J. Colloid Interf. Sci. 333 (2009) 14–26.
[34] J.W. Lee, S.Y. Kim, Y.M. Lee, K.H. Lee, S.J. Kim, Synthesis and characteristics of interpenetrating polymer network hydrogel composed of chitosan and poly(acrylic acid), J. Appl. Polym. Sci. 73 (1999) 113–120.
[35] A. Li, A. Wang, J. Chen, Studies on poly(acrylic acid)/attapulgite superabsorbent composites. II. Swelling behaviors of superabsorbent composites in saline solutions and hydrophilic solvent–water mixtures, J. Appl. Polym. Sci. 94 (2004) 1869–1876.
[36] Y. Zheng, P. Li, J. Zhang, A. Wang, Study on superabsorbent composite. XVI. Synthesis, characterization and swelling behaviors of poly(sodium acrylate)/vermiculite superabsorbent composites, Eur. Polym. J. 43 (2007) 1691–1698.
[37] D. Karadag, S. Tok, E. Akgul, M. Turan, M. Ozturk, A. Demir, Ammonium removal from sanitary landfill leachate using natural Gördes clinoptilolite, J. Hazard. Mater. 153 (2008) 60–66.
[38] I.D. Mall, V.C. Srivastava, G.V.A. Kumar, I.M. Mishra, Characterization and utilization of mesoporous fertilizer plant waste carbon for adsorptive removal of dyes from aqueous solution, Colloids Surf. A 278 (2006) 175–187.